

Mukminov I.R.

*YuganskNIPIneft, Ufa Branch*

## **FILTRATION VELOCITY FIELD IN THE ELLIPTICAL RESERVOIR DRAINED BY A HORIZONTAL WELL**

### **INTRODUCTION**

In the process of calculating field development parameters, specialists use solutions of hydrodynamic problems concerning fluid influx to wells draining the reservoir. Oil pool contours are often schematized by a circle, an ellipsis, a rectangle, a stripe, or by some other geometrical figure. In subsurface hydrodynamics, problems of fluid influx to wells located in a circular or strip reservoir are solved to a greater extent. Using them for the calculation of development parameters automatically schematizes the actual deposit by a corresponding reservoir. Therefore, solutions of fluid influx (particularly in the elliptical reservoir) are interesting from the theoretical and practical points of view.

By the elliptical reservoir we mean a productive reservoir restricted by a horizontal impermeable top and bottom and an elliptical cylinder, which serves as the external boundary of the reservoir.

### **PROPOSED METHOD**

The problem is formulated as follows. It is necessary to find a velocity field of steady-state fluid filtration to a horizontal well, which length is  $\ell_0 = 2\ell$  and the radius is  $r_c$ . The well is located in an elliptical homogeneous-anisotropic ( $\chi$  is the characteristic of vertical anisotropy) reservoir with thickness  $h$  along the bigger axis of the ellipsis. Distances from the well center to its ends are  $g$  and  $f$  (fig.1). The smaller and the bigger semi-axes of the ellipsis are  $a$  and  $b$ . Constant velocity potentials  $\varphi_E$  and  $\varphi_w$  are maintained on the external boundary of the reservoir and on the well side respectively. Filtration is subject to the Darcy law.

If applied to the gallery, this task is partially solved in papers [1,2,3] by means of conformal imaging. Paper [4] shows that if  $\chi h/b > 0.05$ , which is observed in most cases, the fluid influx to the horizontal well with a minimal error in the rate and pressure can be interpreted as the fluid influx to a perfect gallery; at the same time the error in the rate, caused by the substitution of the horizontal well with a perfect gallery does not exceed 5%. Ignoring this error here, we think that the fluid filtration repeats itself in every horizontal layer of the filtration unit element.

Let's use these results and refer the inquisitive reader directly to the sources, giving here the calculation chart only.

$$z_1 = \frac{z + \sqrt{z^2 - c^2}}{c}, \quad c = \sqrt{a^2 - b^2}, \quad (1)$$

$$z_2 = \ln z_1, \quad (2)$$

$$z_2 = \frac{\pi}{2kK(k)} \int_1^w \frac{dw}{\sqrt{(w_B^2 - w^2)(w^2 - 1)}} \Leftrightarrow w = \operatorname{sn} \left[ K(k) + i \frac{2K(k)z_2}{\pi}, k \right], \quad (3)$$

$$\frac{K(k')}{K(k)} = \frac{\ln \frac{a+b}{a-b}}{\pi}, \quad k = \sqrt{1 - k'^2} = \frac{1}{w_B},$$

$$\omega = -i \int_{w_G}^w \frac{(\varphi_K - \varphi_C) \sqrt{(w_B - w_G)(w_F + w_B)} dw}{2K(\lambda) \sqrt{(w_B - w)(w_F - w)(w - w_G)(w + w_B)}} + \varphi_W + i\psi_0, \quad (4)$$

$$\psi_0 = (\varphi_E - \varphi_W) \frac{K(\lambda')}{K(\lambda)}, \quad \lambda' = \sqrt{\frac{2w_B(w_F - w_G)}{(w_B - w_G)(w_F + w_B)}}$$

Here  $K(k)$  is a complete elliptic integral of first kind;  $k$  is the modulus;  $\operatorname{sn}(z,k)$  is the elliptic sinus of Jacoby;  $z$  is the argument [5,6].

Equations (1) - (4) determine the functions that provide necessary conformal images to solve the task in question (fig.1-5).

The distribution of velocity potential  $\varphi$  in rectangle BCGF in the complex plane  $\omega$  is apparently determined by a real component of the complex variable  $\omega = \varphi + i\psi$ .

The following formula holds true for the complex velocity in the plane  $z$ :

$$V_Z = -\frac{d\varphi}{dz} = -\frac{d\varphi}{d\omega} \frac{d\omega}{dw} \frac{dw}{dz_2} \frac{dz_2}{dz_1} \frac{dz_1}{dz} = -\frac{d\varphi}{d\omega} \frac{d\omega}{dw} \frac{1}{\frac{dz_2}{dz_1} \frac{dz_1}{dz}}. \quad (5)$$

Having differentiated expressions (1), (2), (3) and (4), after substituting them into the right part of equation (5) and conducting evident transformations afterwards, we derive the following equation:

$$V_Z = \frac{K(k)(\varphi_K - \varphi_C)}{\pi K(\lambda)} \sqrt{\frac{(1 - kw_G)(1 + kw_F)(1 - w^2)}{(w_F - w)(w - w_G)(z^2 - c^2)}} \quad (6)$$

Let's transform the expression obtained. Separating the real and the imaginary parts in equation (1), we derive

$$z_1 = A + i \cdot B,$$

$$\text{where } A = \frac{x}{c} + \frac{1}{c} \sqrt{\frac{C+D}{2}}, \quad (x \geq 0) \quad A = \frac{x}{c} - \frac{1}{c} \sqrt{\frac{C+D}{2}}, \quad (x < 0)$$

$$B = \frac{y}{c} + \frac{1}{c} \sqrt{\frac{C-D}{2}}, \quad (y \geq 0) \quad B = \frac{y}{c} - \frac{1}{c} \sqrt{\frac{C-D}{2}}, \quad (y < 0)$$

$$C = \sqrt{(x^2 + y^2 + c^2)^2 - 4x^2c^2}, \quad D = x^2 - y^2 - c^2.$$

Further, taking into account the above, we obtain the following expression from the equation (2)

$$z_2 = E + i \cdot F,$$

where  $E = \frac{1}{2} \ln \sqrt{A^2 + B^2}$ ,  $F = \arctg \frac{B}{A}$ .

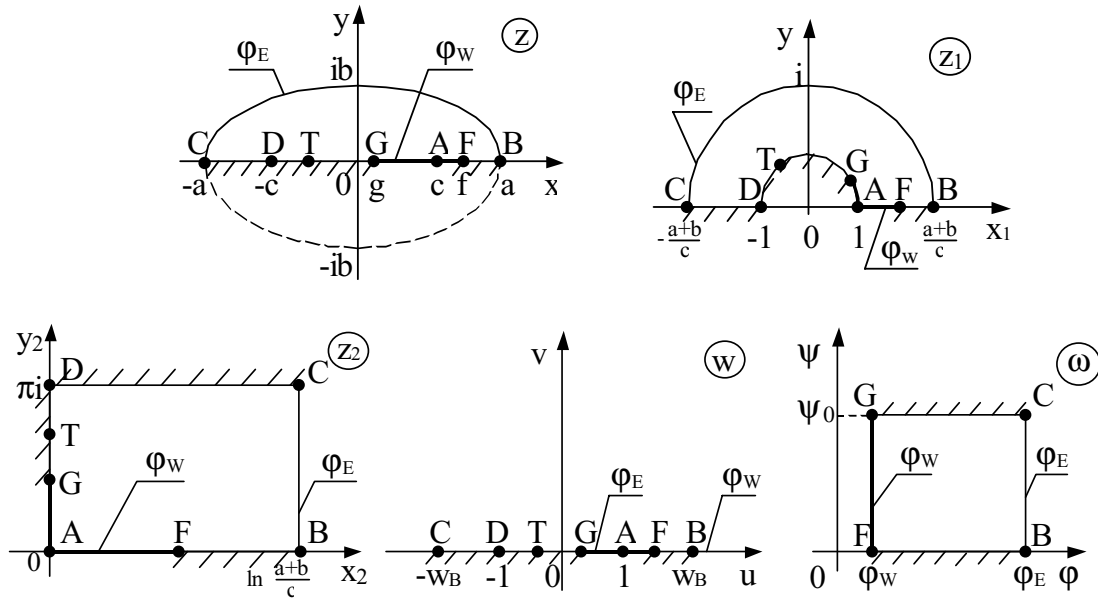


Figure 1 – 5

Then, separating the real and the imaginary parts in the right part of the second equation in system (3) we derive

$$w = G + i \cdot H,$$

where  $G = \frac{\text{sn}(\alpha, k) \text{dn}(\beta, k')}{\text{cn}^2(\beta, k') + k^2 \text{sn}^2(\alpha, k) \text{sn}^2(\beta, k')}$ ,  $H = \frac{\text{cn}(\alpha, k) \text{dn}(\alpha, k) \text{sn}(\beta, k') \text{cn}(\beta, k')}{\text{cn}^2(\beta, k') + k^2 \text{sn}^2(\alpha, k) \text{sn}^2(\beta, k')}$ ,

$$\alpha = K(k) \left( 1 - \frac{2F}{\pi} \right), \quad \beta = \frac{2K(k)E}{\pi}.$$

Let's separate the real and the imaginary parts of the radicand in the right part of the equation (6). We obtain:

$$\sqrt{\frac{1 - w^2}{(w_F - w)(w - w_G)(z^2 - c^2)}} = X + i \cdot Y,$$

where  $X = \frac{1}{\sqrt{2}} \sqrt{\sqrt{R^2 + W^2} + R}$ ,  $Y = -\frac{1}{\sqrt{2}} \sqrt{\sqrt{R^2 + W^2} - R}$ ,

$$R = \frac{PM + QN}{M^2 + N^2}, W = \frac{QM - PN}{M^2 + N^2},$$

$$P = 1 - G^2 + H^2, Q = -2GH, M = SU - TV, N = SV + TU,$$

$$S = w_F G - w_F w_G - G^2 + w_G G + H^2, T = H(w_F - 2G + w_G),$$

$$U = x^2 - y^2 - c^2, V = 2xy.$$

Taking into account the results obtained, the expression (6) for the complex velocity is transformed into the following one:

$$V_Z = V_X + i \cdot V_Y, \quad (7)$$

where  $V_X = CX, V_Y = CY, C = \frac{K(k)(\varphi_E - \varphi_W)\sqrt{(1 - kw_G)(1 + kw_F)}}{\pi K(\lambda')}$ .

Therefore, the formula (7) strictly determines the velocity field in the elliptical reservoir drained by the gallery, which is arbitrarily located along its bigger axis. In case of a horizontal well, the velocity field is determined by the formula (7) with a minimal error in most realizable cases [4].

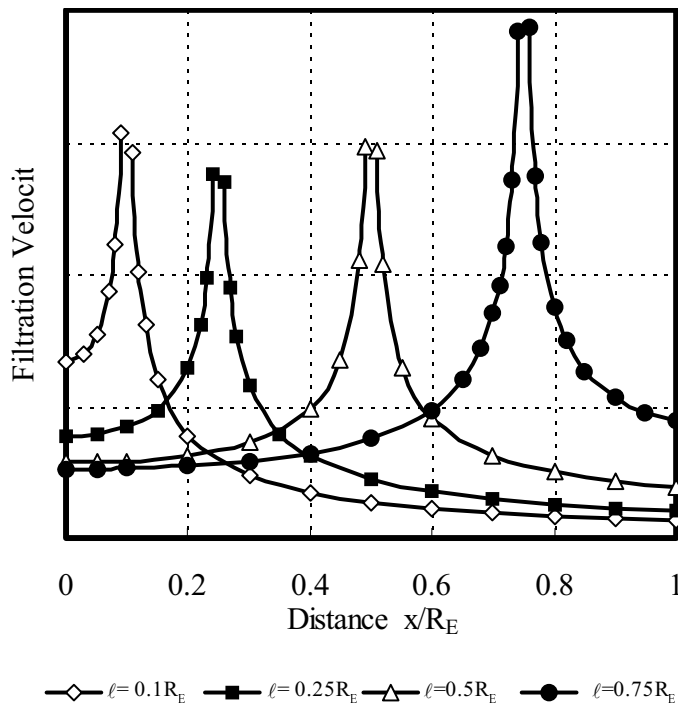


Figure 6

Fig. 6 shows filtration velocity distribution along the diameter of the circular reservoir ( $R_E$  is the radius of external boundary of the reservoir), which is parallel to the symmetrically located gallery draining the reservoir, at various lengths of the gallery. It is clear from the figure that the filtration velocity is maximal (at the limit – infinitely large) in the “end” points of the gallery.

The minimal velocity of filtration is noted on the external boundary of the reservoir. It is characteristic that the filtration velocity in the center of reservoir practically does not depend upon the gallery length at  $l \geq 0.5R_E$ .

The minimal velocity of the fluid influx directly along the gallery is observed in its center. At the same time the average intensity of the fluid influx, f.i. for 10% of the gallery length close to its endings, exceeds the analogous parameter in the central part approximately 3 times. Furthermore, an inverse relation connects the filtration velocity in the center of the gallery with its length: as the gallery

length grows, the velocity falls. This circumstance shows an absolute advantage of horizontal wells (the gallery being their prototype) over vertical wells in deposits with bottom water and/or a gas cap (coning), in incompetent rock (rock destruction in the bottom-hole zone and sand production) and in naturally fractured reservoir rock (the increase in hydrodynamic resistance due to the influence of inertial forces).

Besides, note that at the gallery length  $2\ell \geq R_E$  the intensity of the fluid influx for  $2/3$  of the total length is nearly constant.

Figures 7–9 show the distributions of filtration velocity in a circular reservoir with radius  $R_E$ , drained by a single gallery with lengths  $0.1R_E$ ,  $0.25R_E$  and  $0.75R_E$  respectively. Note, that the distribution of filtration velocity resembles the distribution of the pressure in an infinitely large reservoir drained by two vertical production wells, where, as it is known, the so-called Cassini ovals serve as equipotentials.

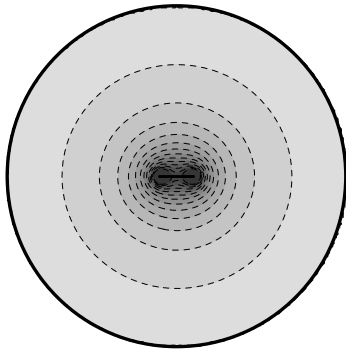


Figure 7

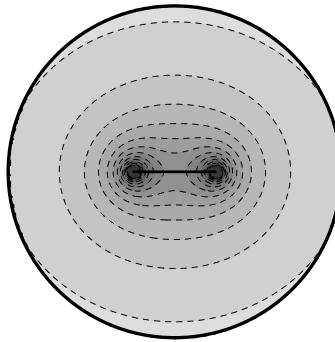


Figure 8

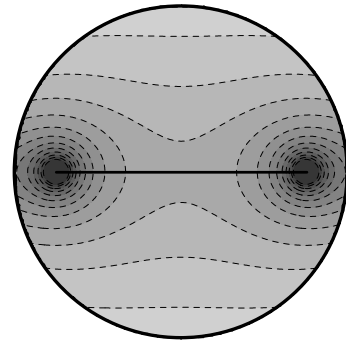


Figure 9

Then, it is clear from fig.7 that when the gallery's half-length is small ( $\ell \leq 0.1R_E$ ), the filtration flow is close to the radial one at such a distance from the gallery, when it exceeds  $2\ell$ , and the lines of equal velocities are nearly concentric circles. It is evidently a manifestation of the empirical regularity, which is well known in the tube hydraulics. According to this regularity the disturbance in the fluid influx, caused by an indirect excitation (under the condition when the geometric size of the body is significantly smaller than the tube diameter) is noticeable if it is located at a distance not exceeding 2-3 of its calibers.

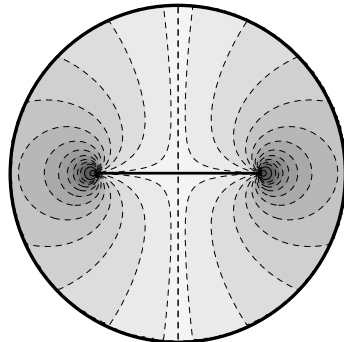


Figure 10

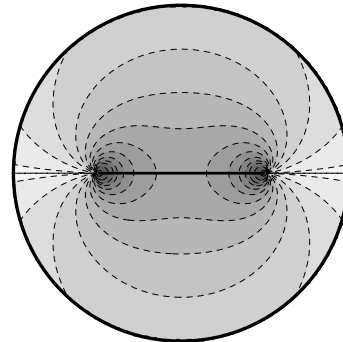


Figure 11

Figures 10 and 11 show the distributions of filtration velocity respectively in the direction of the gallery (along the abscissa axis) and at right angle to it (along the ordinate axis) at  $\ell = 0.5R_E$ . It is clear that in the central part of the reservoir ( $-0.5\ell \leq x \leq 0.5\ell$ ) there is nearly no filtration along the abscissa axis, and the filtration flow here can be considered a linear-parallel one.

Figures 7-11 allow the confirmation of the application validity of some express methods used for rate calculation of the horizontal well. In accordance with these methods the filtration flow is considered a superposition of three constituting basic filtration flows: a linear-parallel one, which flows towards the central part, and two radial flows, which flow to the endings of the horizontal well. Distribution of filtration velocities in the reservoir drained by the gallery (which is a prototype of the horizontal well) are presented in these figures, and they show that such an approach to simulating the influx to the horizontal well is quite suitable for rough, “guess” rate estimations of middle-long and long ( $\ell \geq 0.2R_E$ ) horizontal well.

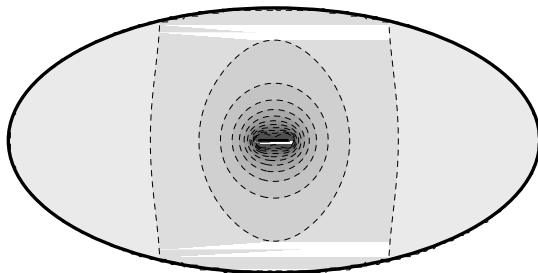


Figure 12

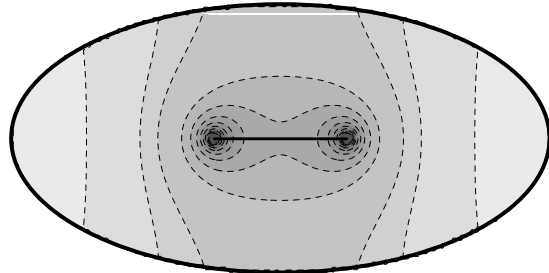


Figure 13

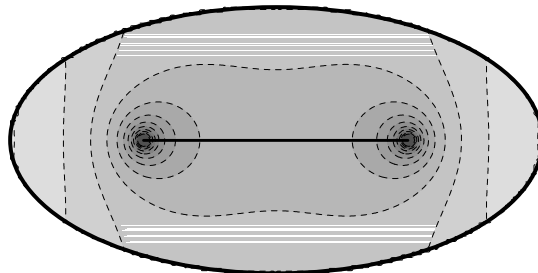


Figure 14

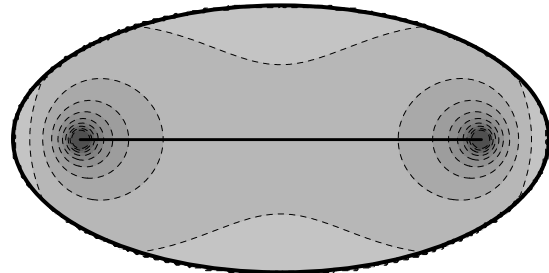


Figure 15

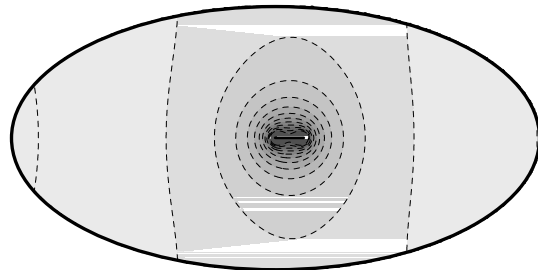


Figure 16

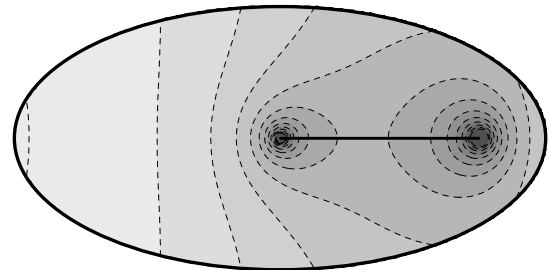


Figure 17

The distribution of filtration velocity in a prolate elliptical reservoir ( $a = 2b$ ) is presented in figures 12-15. Note, that the velocity distribution in the immediate proximity to the gallery is similar to that in a circular reservoir. Principal differences show as we move away from the gallery. Thus, close to the external boundary of the reservoir, the lines of equal velocities look like ovals, at the same time the bigger axis of these ovals is at a right angle to the gallery and to the bigger axis of the external elliptical boundary of the reservoir.

Figures 16-17 reflect the influence of the asymmetry of the gallery location with respect to the external boundary of the reservoir upon the filtration field. It has been assumed for the calculation that the left end of the gallery is located in the central part of the reservoir ( $x = 0, y = 0$ ). It is clear from the figures that when the gallery length is small ( $\ell \leq 0.2b$ ), the influence of such an asymmetry upon the distribution of fluid filtration velocity in the reservoir is insignificant. As the gallery length grows, the influence of its location with reference to the external boundary of the reservoir begins to show even in the immediate proximity to the gallery.

## CONCLUSIONS

- The filtration velocity is maximal in the “end” points of the horizontal well.
- The filtration velocity on the external boundary of the reservoir at  $\ell < 0.5R_E$  and in the center at  $\ell > 0.5R_E$  practically does not depend upon the horizontal well length.
- In case of circular reservoir the filtration flow is close to the radial one and the lines of equal velocities are nearly concentric circles, when the length of horizontal well is small. For middle-long and long horizontal well the filtration flow can be considered as a superposition of three constituting basic filtration flows: a linear-parallel one, which flows towards the central part, and two radial flows, which flow to the endings of the horizontal well.

## REFERENCES

1. Mukminov I.R., Salimgareyev T.F. Fluid influx to the horizontal well in the elliptical reservoir. Scientific and technical conference of student, graduate students and young scientists, #48. Ufa State Petroleum Technological University, 1998.
2. Mukminov I.R. Study of the steady-state influx of fluid to the horizontal well in the elliptical reservoir.- Report theses, International conference #5 “Cybernetic methods of chemical-and-technological processes”. Publishing house of Ufa State Petroleum Technological University, 1999.
3. Mukminov I.R., Salimgareyev T.F. Influence of reservoir external boundary configuration upon horizontal well rate. Scientific and technical conference of student, graduate students and young scientists, #51. Publishing house of Ufa State Petroleum Technological University, 2000.
4. Mukminov I.R. Fluid influx to the horizontal well in the anisotropic reservoir of finite thickness. “Neftepromislovoye delo”, #2, 1999.

5. Gradshteyn I.S., Ryzhik I.M. Tables of integrals, sums, series and products. – M.: Fizmatgiz, 1962. – 1100 pp.

6. E. Yanke, F. Emde, F. Lesh. Special functions. – M.: Nauka, 1968. – 344 pp.